Scripta Materialia 144 (2018) 18–21

Contents lists available at ScienceDirect

Scripta Materialia

journal homepage: www.elsevier.com/locate/scriptamat

Regular article

Current density effects on the microstructure of zirconium thin films

Zahabul Islam, Baoming Wang, Aman Haque *

Department of Mechanical & Nuclear Engineering, 314 Leonhard Building, Pennsylvania State University, PA 16802, USA

ARTICLE INFO

Article history:
Received 17 July 2017
Received in revised form 24 August 2017
Accepted 19 September 2017
Available online xxxx

Keywords:
In-situ TEM
Molecular dynamics
Grain growth
Electron wind force
Grain boundary

ABSTRACT

We investigate the effect of electrical current density below the electromigration failure limit in nanocrystalline zirconium thin films using in-situ Transmission Electron Microscope and molecular dynamics simulation. At least one order of magnitude higher growth was seen at current density of 8.5×10^5 A/cm^2 (Joule heating temperature 710 K) in 15 min compared to conventional thermal annealing at 873 K for 360 min. Simulation results support our hypothesis that the concurrent effects of electron wind force and Joule heating specifically target the grain boundaries, producing much higher grain boundary mobility compared to high temperature annealing alone.

Metallic materials show strong grain size dependence of their properties [1,2] across length scales [3], which has motivated the pursuit for microstructural optimization and control. Thermal annealing is one of the oldest example, where temperature is used as the stimulus for controlling grain size, phases and defect density. For most metals, this temperature is in the range of 0.3–0.4 T_m (where T_m is the homologous temperature). The applied temperature field is uniform, targeting both crystalline and defective regions. The process is time consuming in each of the phases of heating, temperature hold and cooling. This study proposes that electrical current could potentially achieve similar or higher grain boundary and defect mobility at lower energy and time input. This is because of pronounced scattering at the grain boundaries and defect sites [4,5], effectively enhancing atomic mobility exactly where it is needed for grain growth, and not uniformly across the material.

Current density effects are typically studied for degradation through electromigration [5,6]. Beyond a critical density, mass transport takes place due to the electron momentum transfer, particularly intensified at the defective areas. While it is unlikely that electrical annealing will replace conventional thermal annealing in the near future, we argue that its potential for higher atomic mobility is worth investigation at lower current densities. Other studies have focused on electro-plasticity [7], a phenomenon where electrical current flow induces plasticity in materials that are otherwise very hard and brittle. To study the fundamentals of electron transport effects on microstructures, we adopt a combined experiment-simulation approach. The experiments are performed inside a Transmission Electron Microscope (TEM). The high resolution imaging and diffraction modes make TEM first choice in visualization and characterization of microstructural changes (Zheng et al. [8]). The challenge in this technique is the very small work envelope of the TEM chamber, typically accommodating 3 mm diameter grids for specimens [9]. Computational modeling, such as molecular dynamic (MD) simulation has been used to study mechanical properties [10–12] and electro-migration failure [13]. The modeling challenges are in incorporating electron-matter interaction during transport directly. In our MD modeling approach, we represent the effect of the electrical current by applying an equivalent electron wind force and observe the resulting atomic/defect migration. The discrepancy in time and length-scales between experiment and modeling makes it impossible to achieve quantitative agreement. We therefore seek qualitative and mechanistic contributions from the computational modeling efforts to elucidate the experimental observations.

In this present study, we demonstrate the grain growth mechanism due to the electrical current flow in zirconium thin films. Zirconium is a transition metal with a hexagonal closed pack (hcp) lattice structure known for high melting point (2128 K), biocompatibility, good corrosion and radiation resistance, making it a popular choice in nuclear, aviation and surgical implant applications. We first evaporate about 140 nm thick, 99.97% pure zirconium films on silicon-on-insulator (SOI) substrates. The as-deposited films show near- amorphous structure. SOI substrate is used to co-fabricate a micro-electro-mechanical (MEMS) device with the specimen. The specimen is about 100 μm long, 5 μm wide. Standard photo-lithography, lift-off and deep reactive ion etching were performed on the wafer so that the actuator and heater structures were co-fabricated with the specimen which ensures perfect specimen alignment and gripping. Details of the device design and fabrication are given elsewhere [14]. Fig. 1a shows the zirconium thin film on MEMS device, where the heavily doped silicon structures act as electrodes. The device fits a TEM specimen holder with electrical biasing

* Corresponding author.
E-mail address: mah37@psu.edu (A. Haque).

https://doi.org/10.1016/j.scriptamat.2017.09.032
1359-6462/

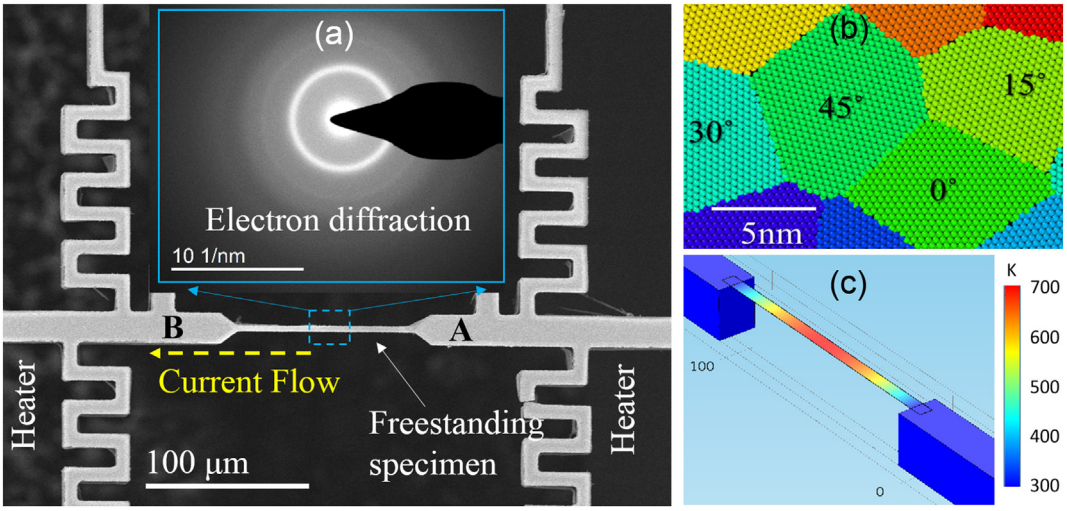

Fig. 1. TEM and MD experimental setups, (a) Scanning electron micrograph of the MEMS device showing the current flow through the specimen. Inset shows diffraction pattern at 0 A/cm^2 current density. (b) Atomistic simulation cell with grains oriented at different angles. (c) Multiphysics simulation of sample with actual geometry, resistance and current density.

capability. In a typical experiment, we pass electrical dc current through the electrodes A and B (as shown in Fig. 1a) to conduct the electrical annealing without damaging the specimen. The inset of Fig. 1a shows the TEM diffraction pattern of a specimen before passing electrical current, where the completely diffused rings suggest near-amorphous (<5 nm grain size) microstructure. Accordingly, the ten grain MD simulation specimen (Fig. 1b) cell was prepared with similar grain size but different orientations. We also performed multi-physics simulation of the temperature field due to Joule heating using COMSOL®. In the in-situ TEM experiments, we passed dc current through the specimen. Since TEM cannot measure temperature field, this information was obtained from multiphysics simulation of the specimen with actual geometry, resistance and current density. Fig. 1c shows the temperature profile along the specimen at a current density of 8.5×10^5 A/cm^2 under vacuum condition mimicking the TEM chamber. The highest temperature is about 710 K and is seen in the middle section of the specimen.

The grain growth mechanism in zirconium due to the electrical current flow was studied using classical MD simulation conducted by LAMMPS [15] software using Embedded Atom Method (EAM) potential [16]. We used a time step of 0.5 fs. Voronoi tessellation based simulation cells of hcp zirconium were built with 10 numbers of grains with an average size of 8 nm. These grain sizes were chosen to mimic the as-deposited specimen as well as grain size distribution in the earlier phases of electrical annealing. We also orient the grain at different angle such as 0°, 5°, 10°, 15°, 30°and 45° as shown in Fig. 1b, while 0° angle lies along [$1\bar{2}10$] direction and [0001] direction corresponds to film normal i. e., c-axis. The model was checked for any overlapping of atoms at the grain boundaries. Energy minimization was carried out using conjugate-gradient (CG) method followed by NPT dynamics for several thousand steps in LAMMPS. To indirectly model the electrical current effects, we apply equivalent wind force on each atom, obtained from the Huntington-Grone [17] ballistic model. The electron wind force on each atom is calculated using the following equations [18]:

$$F_{wind} = Z^* \times e \times j \times \rho \quad (1)$$

where, Z^* is effective valence number, e is electron charge, j is the current density and ρ is the specific resistivity of zirconium. In our present simulation, we consider Z^* as 3.4 [19] and ρ as 421 n$\Omega\cdot$m [20]. During our simulation, we maintained periodic boundary conditions in all directions. Verlet algorithm was employed for time integration during the NPT dynamics. Electron wind force was applied on individual atom followed by energy minimization and NPT dynamics run. We conduct our simulation at 710 K considering Joule heating effect during the current flow through the sample.

Fig. 2 shows the experimentally observed grain growth during the dc current passage through the specimen inside a Tecnai LaB_6 TEM. We allowed 5 min between two consecutive current increments. It is possible to induce grain growth at lower current density at the expense of significant amount of time. Thus, our experimental results can be considered to be at accelerated electrical loading conditions. During the experimentation, we also take TEM BF and selected area electron diffraction (SAED) to probe the grain growth. Fig. 2a–c show the TEM BF and associated SAED images on the microstructural evolution. Starting from near-amorphous grains, we observed very fast grain growth around current density of 8.5×10^5 A/cm^2 (Fig. 2b), where the microstructural changes were discernible within time increments of few minutes. Accelerated loading at current density of 1.1×10^6 A/cm^2 led to vigorous grain growth, discernible in few seconds. Fig. 3b and e show the TEM diffraction patterns for the initial and final conditions in only 15 min time span. The clearly resolved spots in Fig. 3e represent the grain growth similar to that seen in the bright field images.

To assess the effectiveness of electrical current annealing, we also performed thermal annealing on specimens. To see any appreciable growth, we had to anneal the specimen at 873 K with total processing time of 360 min (equal heating, holding and cooling period of 120 min). The process was very slow, taking 24 times as much time as allowed in the current annealing experiment. Fig. 3 shows the comparative picture, clearly showing current annealing to produce at least one order of magnitude larger grain size. This is also reflected by the more resolvable spots in Fig. 3e compared to Fig. 3b, where the diffraction pattern of thermally annealed specimen shows only diffused ring patterns. Finally, absence of any damage in Fig. 3d confirms that electrical annealing can take place below the electro-migration failure current density threshold.

To explain the observed performance, we hypothesize that current annealing efficiently annihilates defects and dislocations localized around defective regions such as grain boundaries. Electrical current annealing involves both electron wind force (electron momentum transfer occurring at defect (vacancy, dislocation, grain boundaries and triple points) and Joule heating ([21,22]). It is well known that grain boundary (GB) atoms are relatively at higher energy state than the equilibrium. This is due to the strain field associated with the defects. Therefore, the momentum transfer effect is more pronounced at the GB region. It is important to distinguish this effect from Joule heating, which arises due to the solids resistance to electron flow. Joule heating also

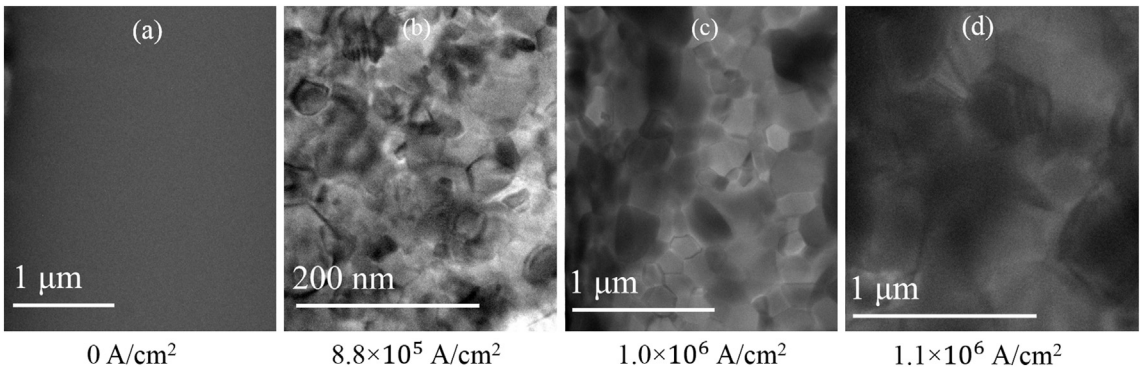

Fig. 2. In-situ TEM study of grain growth as a function of dc electrical current density.

contributes to the enhanced atomic mobility – however, it is uniform in nature and cannot specifically target GBs or other defects. In a similar fashion, conventional thermal annealing involves heating of both GB and grain interior. In bulk metals, the volume fraction of GB is <5%, therefore thermal annealing is sub-optimal from energy consumption and time perspective. Electrical annealing, on the other hand, is more localized at the GB regions (just where needed) and thus can potentially be more time and energy efficient.

To obtain a qualitative validation of our hypothesis, we performed MD simulation that indirectly captures current flow effect by imposing the electron wind force. Fig. 3c and f show simulation cell after thermal and electrical annealing respectively. The electrical annealing was conducted for 25 ps followed by energy minimization and 50 ps NPT dynamics run whereas thermal annealing was conducted for 1.1 ns, which is 20 times higher than the electrical annealing time. However, total thermal annealing takes 1.1 ns, which includes first stage heating from 300 K to 873 K with a temperature ramp rate of 0.012 K/fs, second stage annealing by holding temperature at 873 K for 1.0 ns and final stage cooling from 873 K to 300 K at a cooling rate of 0.012 K/fs. We then equilibrate the system for 100 ps at room temperatures i.e. 300 K. Thermal annealing occasionally led to grain boundary reconstruction (indicated by arrows in Fig. 3c), while other grains remain at the original state.

The MD simulation allows us to investigate our hypothesis at the atomic level. It is evident from Fig. 3f that atomic re-orientation and diffusion are dominant at grain boundaries during the flow of current. The significant grain growth transforms the nanocrystalline specimens to a single crystal with a few minor defect sites. The disappearance of the grain boundaries is seen to be a result of diffusional motion of the defects under the impetus of the electron wind force. Fig. 4a shows that the grain boundaries experience localized stress field, which could be attributed to the local defects in atomic position, orientation and defect density at grain boundaries. The localized stresses in the grain boundary regions also indicate higher potential energy states compared to atoms at grain interior. The mechanical stress field around the defects is another reason behind the localized and targeted atomic mobility increase at the grain boundaries. Due to the imparted electron wind forces on atoms, an elastic stress develops on the simulation cell. Based on Eq.

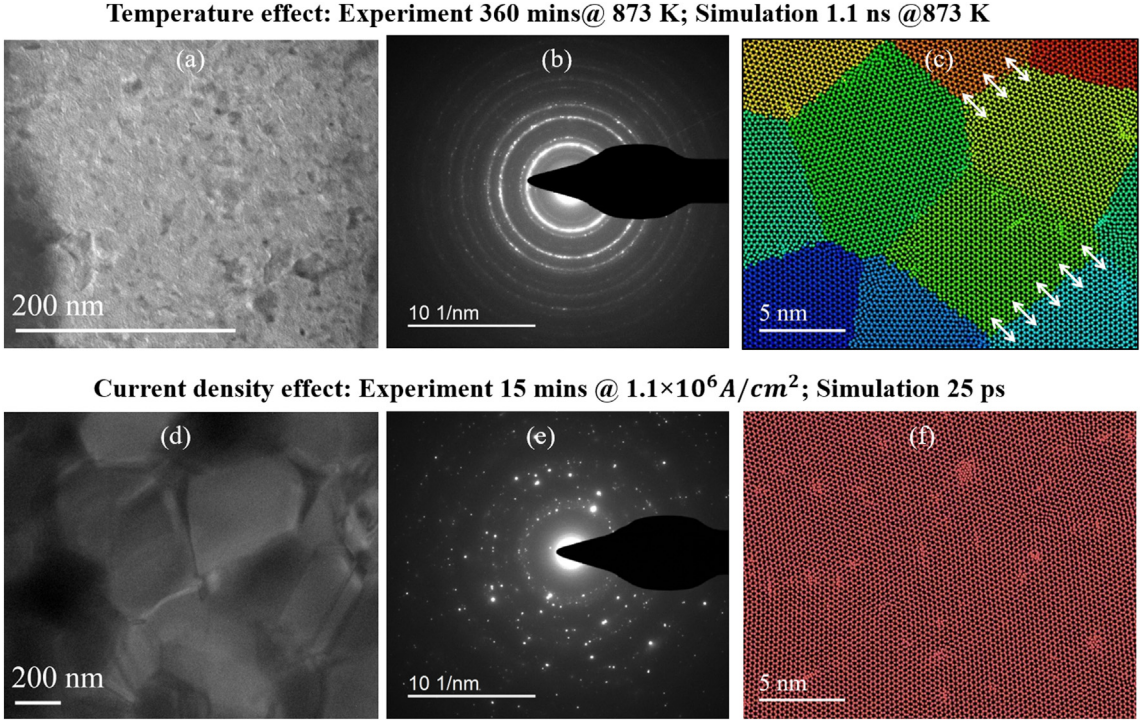

Fig. 3. Comparison between thermal and electrical annealing, (a) TEM bright field image after temperature loading (b) corresponding electron diffraction (c) MD simulation showing grain boundary reconstruction in limited locations indicated by arrows (d) TEM bright field image after current loading (e) corresponding electron diffraction (f) MD simulation showing pronounced grain growth due to the electrical current loading.

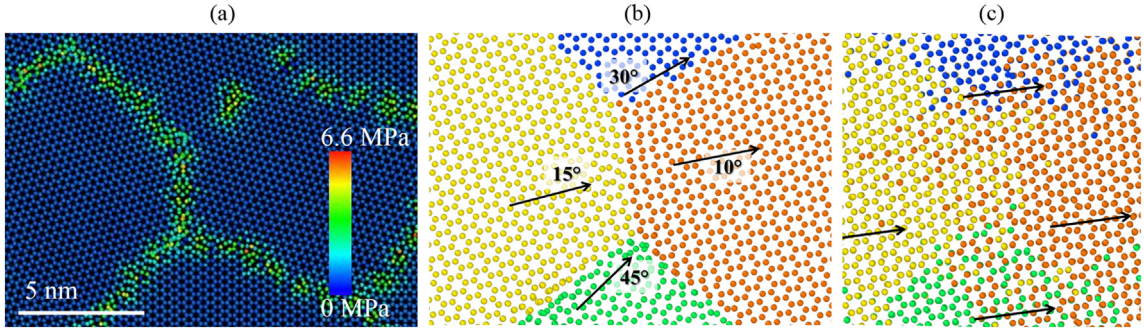

Fig. 4. MD simulation trajectory shows time evolution of grain growth (a) initial structure. (b) grain growth after 15 ps electrical annealing. (c) two triple points before electrical annealing. (d) two triple points of hcp zirconium after annealing respectively.

(1) the calculated wind force is 77.5 pN and this equivalent wind force develops an elastic stress of 3.95 MPa on the simulation cell. This additional elastic stress assists GB migration due to elastic anisotropy of Zr. The enhanced mobility allows atoms to relax and reorient to achieve minimum energy state. This atomic mobility and relaxation at the grain boundaries further leads to the grain growth. Fig. 4b and c show an extended view of two triple points. Fig. 4b shows two triple points with initial orientation of four grains at 10°, 15°, 30° and 45° as indicated by arrows. After electrical annealing, we notice grain boundaries disappeared as shown in Fig. 4c. The reconstruction of original hcp-crystalline structure of zirconium from different grain sites (as shown in Fig. 4c) clearly indicates that the grains grow in zirconium thin film due to the strong interaction between electrical wind force and diffusing atoms at the grain boundaries. We also notice that atoms from one grain diffuse to another grain, which provides an evidence of higher mobility of atom due to the pronounced electron scattering at the grain boundaries. In addition to this, we also notice that after electrical annealing all the grain boundaries are oriented along the same direction (~0°) as shown by arrows in Fig. 4c. All of these phenomena indicate that electrical current could significantly increase the grain size in thin films.

In summary, we performed in-situ TEM experiments on near-amorphous zirconium thin films to obtain fundamental understanding behind electrical current density induced grain growth. About two orders of magnitude grain growth was observed in <15 min at a current density of 8.5×10^5 A/cm^2 and accompanied Joule heating temperature of 710 K. This was about one order of magnitude higher than what we observed in similar specimens but under convention thermal annealing at 873 K for 120 min. We performed MD simulation to show that the effect of electron wind force is to impart very high atomic mobility that is localized to the defects and grain boundaries. This has the potential be more energy efficient compared to the thermal annealing where the crystalline grain interiors are heated to the same temperature as the defective areas that need recrystallization. Our computational model shows that localized stress fields around the defects further increase the atomic mobility accommodated by diffusion to increase the grain size by annihilating the grain boundaries. The findings of this study may play vital role in developing novel energy and time efficient techniques for microstructural reorganization and control in the future.

We acknowledge the support of the US Department of Energy funding (DE-NE0008259) and from the National Science Foundation (DMR 1609060). The fabrication was performed at the Pennsylvania State University Nanofabrication Facility. All experiments were performed at the Pennsylvania State University Materials Characterization Facility.

References

[1] J.R. Greer, J.T.M. De Hosson, Prog. Mater. Sci. 56 (6) (2011) 654–724.
[2] K.S. Kumar, H. Van Swygenhoven, S. Suresh, Acta Mater. 51 (19) (2003) 5743–5774, https://doi.org/10.1016/j.actamat.2003.08.032.
[3] E. Arzt, Acta Mater. 46 (16) (1998) 5611–5626.
[4] P. Asoka-Kumar, K. O'Brien, K.G. Lynn, P.J. Simpson, K.P. Rodbell, Appl. Phys. Lett. 68 (3) (1996) 406–408 http://dx.doi.org/10.1063/1.116700.
[5] C. Basaran, M. Lin, Mech. Mater. 40 (1) (2008) 66–79.
[6] M.D. Thouless, Scr. Mater. 34 (12) (1996) 1825–1831.
[7] Huu-Duc Nguyen-Tran, Hyun-Seok Oh, Sung-Tae Hong, Heung Nam Han, Jian Cao, Sung-Hoon Ahn, Doo-Man Chun, Int. J. Precis. Eng. Manuf. 2 (4) (2015) 365–376, https://doi.org/10.1007/s40684-015-0045-4.
[8] H. Zheng, A. Cao, C.R. Weinberger, J.Y. Huang, K. Du, J. Wang, Y. Ma, Y. Xia, S.X. Mao, Nature Communications 1 (2011) 144.
[9] B. Wang, M.T. Alam, M.A. Haque, Scr. Mater. 71 (2014) 1–4.
[10] A. Latapie, D. Farkas, Scr. Mater. 48 (5) (2003) 611–615.
[11] C.J. Ruestes, G. Bertolino, M. Ruda, D. Farkas, E.M. Bringa, Scr. Mater. 71 (2014) 9–12.
[12] J. Schiotz, F.D. Di Tolla, K.W. Jacobsen, Nature 391 (6667) (1998) 561–563.
[13] S. Shingubara, I. Utsunomiya, T. Fujii, Electron. Commun. Jpn. 78 (12) (1995) 82–95.
[14] M.A. Haque, M.T.A. Saif, Proc. Natl. Acad. Sci. U. S. A. 101 (17) (2004) 6335–6340.
[15] S. Plimpton, J. Comput. Phys. 117 (1) (1995) 1–19.
[16] M.I. Mendelev, G.J. Ackland, Philos. Mag. Lett. 87 (5) (2007) 349–359.
[17] H.B. Huntington, A.R. Grone, J. Phys. Chem. Solids 20 (1–2) (1961) 76–87.
[18] R.S. Sorbello, A. Lodder, S.J. Hoving, Phys. Rev. B 25 (10) (1982) 6178–6187.
[19] J.P. Dekker, A. Lodder, J. vanEk, Phys. Rev. B 56 (19) (1997) 12167–12177.
[20] P.D. Desai, H.M. James, C.Y. Ho, J. Phys. Chem. Ref. Data 13 (4) (1984) 1097–1130.
[21] H. Conrad, Mater. Sci. Eng., A 287 (2) (2000) 276–287.
[22] Wesley A. Salandro, Joshua J. Jones, Cristina Bunget, Laine Mears, John T. Roth, Electrically Assisted Forming 2014, pp. 37–54, https://doi.org/10.1007/978-3-319-08879-2.